Static and Vibronic Contributions to the Spectral Intensities of Tetrahalocopper(II), -platinum(II), and -palladium(II) Chromophores

Adam J. Bridgeman and Malcolm Gerloch*

University Chemical Laboratories, Lensfield Road, Cambridge CB2 1EW, U.K.

Received January 26, 1995[⊗]

The intensity distributions in the ligand-field spectra of nine planar and "tetrahedral" complexes $[MCl_4]^{2-}$ (M = Pt, Pd, Cu; X = Cl, Br) have been modeled within a cellular ligand-field (CLF) approach. Vibronic sources of parity mixing, providing the whole contribution to intensity in the centric, planar species but a much smaller contribution in the "tetrahedral" species are included for bending vibrations only. Contributions from different bending modes and, as appropriate, from the static field are all related after normal coordinate analysis of vibrational frequencies to four underlying "static" CLF intensity parameters ${}^{P}t_{\sigma}$, ${}^{F}t_{\sigma}$, ${}^{P}t_{\pi}$, and ${}^{F}t_{\pi}$. In fitting intensity *distributions*, only three of these are free variables. All intensity analyses proceeded successfully and briskly to define essentially unique parameter sets. Chemically sensible variations in the parameter values are observed with respect to both geometry and d^n configuration. Comparisons of intensity parametrizations are made here with respect to the larger group of closely related chromophores analyzed by the CLF model to date.

Introduction

In 1988 we introduced our cellular ligand-field (CLF) model[1] of the intensity distributions in the "d−d" spectra of acentric transition metal chromophores. Intensity was deemed to arise through permanent odd-parity admixtures into the nominal d orbitals in noncentrosymmetric systems. Within this "static" approach—model I—local transition moments are parametrized by the quantities ${}^{L}t_{\lambda}$ here $\lambda = \sigma, \pi_x, \pi_y$ in correspondence with CLF energy parameters e_λ. The superscript L = P, F refers to odd-parity admixtures of p or f orbital character. The ratios ${}^{P}t_{\lambda}:{}^{F}t_{\lambda}$ have been shown,[2] theoretically and empirically, to reflect both radial and lateral character of the various metal-ligand bonds in a given chromophore. Intensity distributions in the "d−d" spectra of some 50 transition metal chromophores have been reproduced[3−9] essentially quantitatively, by model I.

A major development[10] of this approach in 1993 provided for the analogous modeling of the "d−d" intensities in centric chromophores in which the required parity mixing arises dynamically during the course of molecular vibrations. Sets of parameters, ${}^{L}t_{\lambda}^{\alpha}(Q)$, for local transition moments are required within this "vibronic" scheme—model IIA—one for each parity mixing brought about by ligand displacement in direction α within the intensity inducing mode, Q. Intensity distributions in the spectra of several crystals containing the centric, planar $[CuCl_4]^{2-}$ ion[11] and[12] of $[PtCl_4]^{2-}$ and $[PtBr_4]^{2-}$ have been modeled within this approach. These analyses were difficult because of the high degree of parametrization required by consideration of several intensity inducing vibrational modes, even though attention was restricted to bends. While satisfactory reproduction of all observed intensity distributions was achieved, considerable ambiguity in optimal parameter values—for the copper systems especially—was apparent. It proved impossible to determine any satisfactorily definitive parametrization of the intensities for the $[PdCl_4]^{2-}$ chromophore whose spectral traces are less well resolved than those of the platinum analogue. Even so, these studies demonstrated a broad efficacy for the approach in that the relative activities of the various inducing modes qualitatively accorded with their known infrared and Raman frequencies.

These successes encouraged us to exploit one further feature of the vibronic model that the ${}^{L}t_{\lambda}^{\alpha}(Q)$ parameters of a bending mode Q are equal to those of an "underlying" static parametrization, ${}^{L}t_{\lambda}$, multiplied by the root-mean-square (RMS) tangential displacements suffered by each ligand within that mode. Within this extended approach[13]—model IIB—ligand displacements are estimated by prior normal coordinate analysis (NCA) of vibrational frequencies. Parametrization of the CLF vibronic model now involves the same number of degrees of freedom as incurred with the original "static" model. Furthermore, in nearly but not exactly centric chromophores, in which significant parity mixing arises both statically and vibronically, analysis of contributions from all sources—static and vibronic from several modes—incurs no higher degree of parametrization. Model IIB has been applied to several $CuCl_2X_2$ chromophores, where X refers to both oxygen and nitrogen donors, all of which are exactly centric,[13] and to $[Nien_3]^{2+}$, whose acentric geometry approaches O_h symmetry somewhat.[14] Excellent reproduction of the experimental intensity distributions has been achieved in each case, and for the $[Nien_3]^{2+}$ chromophore, this success (using just one intensity parameter) included a good account of the circular dichroism also.

It is timely, therefore, to reassess the completed vibronic model in application to the aforementioned planar tetrahalo complexes. The present report addresses four basic issues: (a) the efficacy of model IIB for important, "key", ML_4 chro-

[⊗] Abstract published in *Advance ACS Abstracts,* August 1, 1995.

(1) Brown, C. A.; Gerloch, M.; McMeeking, R. F. *Mol. Phys.* **1988**, *64*, 771.
(2) Brown, C. A.; Duer, M. J.; Gerloch, M.; McMeeking, R. F. *Mol. Phys.* **1988**, *64*, 825.
(3) Brown, C. A.; Duer, M. J.; Gerloch, M.; McMeeking, R. F. *Mol. Phys.* **1988**, *64*, 793.
(4) Duer, M. J.; Fenton, N. D.; Gerloch, M. *Int. Rev. Phys. Chem.* **1990**, *9*, 227.
(5) Fenton, N. D.; Gerloch, M. *Inorg. Chem.* **1989**, *28*, 2975.
(6) Duer, M. J.; Gerloch, M. *J. Chem. Soc., Dalton Trans.* **1989**, 2109.
(7) Duer, M. J.; Gerloch, M. *Inorg. Chem.* **1989**, *28*, 4260.
(8) Fenton, N. D.; Gerloch, M. *Inorg. Chem.* **1990**, *29*, 3718.
(9) Fenton, N. D.; Gerloch, M. *Inorg. Chem.* **1990**, *29*, 3726.
(10) Duer, M. J.; Essex, S. J.; Gerloch, M.; Jupp, K. M. *Mol. Phys.* **1993**, *79*, 1147.
(11) Duer, M. J.; Essex, S. J.; Gerloch, M. *Mol. Phys.* **1993**, *79*, 1167.
(12) Bridgeman, A. J.; Gerloch, M. *Mol. Phys.* **1993**, *79*, 1195.
(13) Bridgeman, A. J.; Gerloch, M. *Inorg. Chem.* **1994**, *33*, 5411.
(14) Bridgeman, A. J.; Gerloch, M. *Inorg. Chem.* **1994**, *33*, 5424.

0020-1669/95/1334-4370$09.00/0

Table 1. Molecules Studied in This Work, Where the Last Four Columns Cite Other Work by Reference Number

abbreviation	compound	refs: IR/Raman	refs: NCA	refs: "d−d" spectra	refs: CLF analysis
	Planar $CuCl_4$ Coordination				
METH	(1-methyl-4-oxo-3,3-diphenylhexyldimethylammonium)$_2CuCl_4$	15, 16	15	15, 16, 25	11, 19
CREAT	(2-imino-1-methyl-4-imidazolinium)$_2CuCl_4$	15, 16		15, 16, 20	11, 19
NMPH	(*N*-methylphenethylammonium)$_2CuCl_4$ (green form)	15, 16, 21	15	15, 21	11, 19
NAEM	*N*-(2-aminoethylmorpholinium)$CuCl_4$ (green form)	15		15, 22, 23	
	Nonplanar $CuCl_4$ Coordination				
Cs_2CuCl_4	Cs_2CuCl_4	24, 17, 18	26	27	28
NBZP	(*N*-benzylpiperazinium hydrochloride)$_2CuCl_4$	15		15, 23	11, 19

Table 2. Molecular Geometries for Planar and Non-Planar $[CuCl_4]^{2-}$ Ion

compound	Cu−Cl bond length (Å)	trans Cl−Cu−Cl angle (deg)	cis Cl−Cu−Cl angle (deg)	ref
METH	2.253, 2.283	180	89.5, 90.5	29
CREAT	2.233, 2.268	180	89.9, 90.1	30
NMPH	2.248, 2.281	180	89.9, 90.1	31
NAEM	2.240, 2.314	180	89.8, 90.2	32
NBZP	2.252, 2.249, 2.334, 2.234	166.6, 166.3	89.8, 91.5, 90.0, 91.8	33
Cs_2CuCl_4	2.224, 2.220, 2.220, 2.235	127, 131	100, 102	26

mophores with geometry variations exemplifying centric planar to more nearly tetrahedral; (b) the clearer definition of parameter values in these species; (c) the analysis of the experimentally less favorable $[PdCl_4]^{2-}$ chromophore; (d) the investigation and exploitation of the known temperature dependence of some of these spectral intensity distributions. Analyses are presented for six tetrachlorocopper(II) systems, four of which are planar and centric and two of which show small and large tetrahedral departures from planarity; and of the d^8 chromophores $[PtCl_4]^{2-}$, $[PtBr_4]^{2-}$, and $[PdCl_4]^{2-}$.

All analyses have been successful. Our earlier conclusions for the $[PtCl_4]^{2-}$ complex are confirmed. Those for the planar copper species are greatly sharpened and important deepening of our understanding of the bonding and significance of CLF intensity parametrization emerges from a comparison of the planar and "tetrahedral" copper species.

Analyses of $[CuCl_4]^{2-}$ Chromophores

In Table 1 we list names and abbreviation for the four planar and two nonplanar tetrachlorocuprates, together with citations to experimental infrared/Raman and "d−d" spectral measurements and to NCA and earlier CLF analyses. Geometrical details of their first coordination shells are listed in Table 2. Up to three transition energies have been determined from two or more spectral polarizations for each chromophore, except NAEM. The NAEM crystals contain both planar and "tetrahedral" $[CuCl_4]^{2-}$ ions in the same lattice. The lower energy band of the planar chromophore overlaps the higher energy band of the "tetrahedral" one; and the bands in the latter are insufficiently well resolved for detailed analysis. Our analysis for the planar chromophore of NAEM, presented here for the first time, is the least detailed of the present set of six, being based upon just two transitions—albeit one in two polarizations, the other in three.

CLF Energy Analyses for the Planar Chromophores. Apart from NAEM, the transition energies have been analyzed within the CLF model before.[11] The spin−orbit coupling coefficient was held fixed at 700 cm^{-1} throughout; several computational checks with our CAMMAG4 program suite[34] using the full ^2D basis, have shown that calculated transition energies (and, later, intensity distributions) are reasonably insensitive to variations of ± 200 cm^{-1} in this value. That leaves just three variables—e_σ(Cl), e_π(Cl), e_σ(void), relating to σ and π Cu−Cl interactions and to the ligand field of each coordination void, above and below the coordination plane. The three spectral bands ν_1, ν_2, and ν_3 correspond to the orbital and term transitions in (1).

$$\begin{aligned} \nu_1: &\quad {}^2B_{2g}(xy) \leftarrow {}^2B_{1g}(x^2-y^2) \\ \nu_2: &\quad {}^2E_g(xz,yz) \leftarrow {}^2B_{1g}(x^2-y^2) \\ \nu_3: &\quad {}^2A_{1g}(z^2) \leftarrow {}^2B_{1g}(x^2-y^2) \end{aligned} \tag{1}$$

The analyses were straightforward and unexceptional. The optimal parameter values and comparisons of observed with calculated transition energies are given in ref 11 for METH, CREAT and NMPH. The transitions ν_2 and ν_3 are observed at approximately 14 850 and 17 290 cm^{-1}, respectively, in the spectrum of NAEM. Using the CLF parameter set e_σ(Cl) = 5520, e_π(Cl) = 870, and e_σ(void) = −2925 cm^{-1}, the transitions energies are calculated to be 12 994 (ν_1), 14 713 and 14 868 (ν_2), and 17 297 (ν_3) cm^{-1}.

CLF Energy Analyses for the Nonplanar Chromophores. Three transitions are also possible for $[CuCl_4]^{2-}$ complexes of D_{2d} symmetry, to which NBZP and Cs_2CuCl_4 approximate. Defining molecular axes with z bisecting the large Cl−Cu−Cl angle and x and y approximately parallel to the projections of the Cu−Cl bonds onto the plane normal to z, we define the three transitions as in (2). The order of ν_1 and ν_2 depends upon

$$\begin{aligned} \nu_1: &\quad {}^2B_1(xy) \leftarrow {}^2B_2(x^2-y^2) \\ \nu_2: &\quad {}^2E(xz,yz) \leftarrow {}^2B_2(x^2-y^2) \\ \nu_3: &\quad {}^2A_1(z^2) \leftarrow {}^2B_2(x^2-y^2) \end{aligned} \tag{2}$$

the magnitude of the distortion from tetrahedral geometry. NBZP is nearly planar, and ν_1 occurs at a lower energy than ν_2. The optimal CLF parameter values and a comparison between observed and calculated transition energies have been previously reported[11] for this complex.

For Cs_2CuCl_4, the order of ν_1 and ν_2 are reversed in this much more nearly tetrahedral molecule. Earlier CLF analyses[35] using only e_σ(Cl) and e_π(Cl) variables defined a value of 33 000 cm^{-1} for Σ, the ligand-field trace (the sum of all e_σ and e_π values) which is out of line with trace values for very many other M(II) complexes. Later it was shown[28] how inclusion of a small value for e_σ(void), in recognition of the two wide Cl−Cu−Cl angles, furnished an equally good fit to the experimental transition

Table 3. Vibrational Frequencies (cm^{-1}) of the Planar $[CuCl_4]^{2-}$ Ions

vibration	symmetry	activity (IR/Raman)		METH	CREAT	NMPH	NAEM
ν_1	a_{1g}	R		275	290	276	*d*
ν_2	a_{2u}	IR		159	150	158	168
ν_3	b_{2g}	R		181	202	182	*d*
ν_4	b_{2u}		i	62[a]	64[a]	64[c]	64[a]
			ii	88[b]	84[b]	84[b]	88[b]
			ii			105[a]	
ν_5	b_{1g}	R		195	*d*	209	*d*
ν_6	e_u(stretch)	IR		303	308	314	318
				285	290	285	276
ν_7	e_u(bend)	IR		179	188	193	208
				177			181

[a] Inactive mode calculated by use of the coth rule.[15,16,21] [b] Inactive mode calculated by setting $F_{22} = F_{44}$ in normal coordinate analysis (text and ref 15). [c] Frequency equal to that obtained for CREAT by use of coth rule. [d] Not observed.

energies but with a much lower value of Σ. A further desired lowering of the trace was found to be possible on recognition of the possibilities for misdirected valency insofar that some small overlap of ligand functions with the $d_{x^2-y^2}$ may be involved. This modeling involves the use of $e_{\pi\sigma}$ and $e_{\pi x} \neq e_{\pi y}$, for the Cu−Cl interactions. It is not possible to define all these parameters from so small a set of observed transitions. The range of possible parameter values are given in ref 28. The parameter set e_σ(Cl) = 4475, $e_{\pi x}$(Cl) = 950, $e_{\pi y}$(Cl) = 750, $e_{\sigma\pi x}$(Cl) = 200, and e_σ(void) = −425 cm^{-1} is exemplary of the situation and is used in the present study. Separate calculations throughout our analyses show that fits to both transition energies and intensity distributions change little with small changes in these CLF energy parametrizations.

NCA of Vibrational Frequencies. Analysis of the vibronic contributions to the "d−d" spectra is predicated upon estimates of ligand displacements from normal coordinate analysis of infrared/Raman vibrational frequencies. As Table 1 shows, NCA studies have already been published for most of the present copper(II) systems. We have extended these to include CREAT, NAEM, and NBZP chromophores. In addition, we report on two or three variations of these NCAs for the planar species as follows. The b_{2u} bending vibration, ν_4, imposing a tetrahedral distortion onto the square planar $[CuCl_4]^{2-}$ framework, is both Raman and infrared inactive and hence unobserved. In Table 3, different estimates for its frequency are entertained. Those labeled (a) were deduced by McDonald and Hitchman[16] by fitting the temperature of the ν_3 "d−d" band, which (on neglect of spin−orbit coupling) is exclusively enabled by the b_{2u} bend, by the usual coth rule approach. Those labeled (b) are calculated from NCA of the ν_2, a_{2u}, bend assuming no coupling between the force constants referring to the "orthogonal" Cl−Cu−Cl bending displacements (i.e. that F_{44} is set equal to F_{22}—see Appendix). Inclusion of the (a) frequencies into the NCAs together with implicit recognition of the coupling between the Cl−Cu−Cl displacements through $F_{44} \neq F_{22}$ yields the F_{44} values given in Table 4. The value of $\nu_4 = 105$ cm^{-1} for NMPH from the coth rule analysis by Hitchman and Cassidy[21] is, as noted by McDonald,[15] out of line with the ν_4 values for the planar chromophores. Accordingly, the vibronic analyses of the ligand-field spectra, described below, have been performed

Table 4. Symmetry Coordinate Force Constants (mdyne $Å^{-1}$) for the Planar $[CuCl_4]^{2-}$ Ions

force constant	METH	CREAT	NMPH	NAEM
F_{11}	1.580	1.980	1.591	
F_{22}	0.082	0.073	0.081	0.091
F_{33}	0.171	0.213	0.173	
F_{44}	0.044[a]	0.043[a]	0.115[a]	0.044[a]
			0.044[b]	
F_{55}	0.795		0.912	
F_{66}	0.970	0.959	1.002	0.989
F_{67}	0.159	0.144	0.172	0.172
F_{77}	0.217	0.244	0.255	0.286

[a] Calculations performed using $F_{22} = F_{44}$. [b] Force constant yielding $\nu_4 = 64$ cm^{-1}.

Table 5. Vibrational Frequencies (cm^{-1}) of the Nonplanar $[CuCl_4]^{2-}$ Ions

vibration	symmetry	NBZP ref 15	force constant (mdyne $Å^{-1}$)	Cs_2CuCl_4 ref 17, 18, 24	force constant (mdyne $Å^{-1}$)
ν_1	a_1(stretch)	274	$F_{11} = 1.568$	280	$F_{11} = 1.639$
ν_2	b_2(bend)	169	$F_{22} = 0.099$	105	$F_{22} = 0.111$
ν_3	b_1(bend)	185	$F_{33} = 0.182$	151	$F_{33} = 0.141$
ν_4	a_1(bend)	80	$F_{44} = 0.068$	103	$F_{44} = 0.111$
ν_5	b_2(stretch)	214	$F_{55} = 0.912$	258	$F_{55} = 0.939$
ν_6	e(stretch)	284	$F_{66} = 0.691$	288	$F_{66} = 0.871$
		292	$F_{67} = 0.177$	296	$F_{67} = 0.023$
ν_7	e(bend)	187	$F_{77} = 0.338$	121	$F_{77} = 0.110$
		197		136	

with two or three sets of RMS ligand displacements, corresponding to the row entries i, ii, and iii in Table 3. Table 5 lists vibrational frequencies and force constants for the nonplanar species NBZP and Cs_2CuCl_4. The force constants in Tables 4 and 5 are defined in the Appendix.

Intensity Analyses for the $[CuCl_4]^{2-}$ Species

The Database. The spectra of METH have been recorded[15,16] at 10, 60, 100, 200, and 290 K for light incident on the (100) crystal face and polarized parallel to *b* and *c*. Intensities were recorded on an absolute scale. Three bands are resolvable at lower temperatures; resolution decreases somewhat with increasing temperatures.

Similar *b* and *c* polarized spectra were recorded[15,16] for the (100) face of CREAT at 10, 50, 90, 140, and 180 K. Once again measurements of crystal thickness have placed the intensities on an absolute scale. Three bands are resolvable at lower temperatures in the *b* polarization; two in *c*. The lowest energy band in *c* polarization appears to have very low intensity. Resolution decreases somewhat with increasing temperature.

For NMPH, crystal spectra for light incident on the (010) face and polarized parallel to the *b* axis and at an angle of 45° to the *a* axis have been recorded[21] at 10, 77, 120, and 185 K. Three transitions are resolvable at each temperature. The spectra at 45° to *a* are labeled POL 1 in the work described below.

The spectra for the $(10\bar{1})$ crystal face of NAEM has been recorded[15,22,23] at 10K for light polarized parallel to *b* and to [010]—hereafter labeled POL 2. The spectrum for light polarized parallel to *c* and incident upon (010) has also been recorded. Intensities have been determined on an absolute scale. These crystals contain both planar and flattened tetrahedral $[CuCl_4]^{2-}$ units, as discussed above. Two bands clearly

(15) McDonald, R. G. Ph.D. Thesis, University of Tasmania, Hobart, 1988.
(16) McDonald, R. G.; Hitchman, M. A. *Inorg. Chem.* **1986**, *25*, 3273.
(17) Dunsmuir, J. T. R.; Lane, A. P. *J. Chem. Soc. A* **1971**, 404.
(18) Dunsmuir, J. T. R.; Lane, A. P. *J. Chem. Soc. A* **1971**, 2781.
(19) Essex, S. J. Ph.D. Thesis, University of Cambridge, U.K., 1992.
(20) Hitchman, M. A. *J. Chem. Soc., Chem. Commun.* **1979**, 973.
(21) Hitchman, M. A.; Cassidy, P. J. *Inorg. Chem.* **1979**, *18*, 1745.
(22) McDonald, R. G.; Riley, M. J.; Hitchman, M. A. *Inorg. Chem.* **1989**, *28*, 752.
(23) McDonald, R. G.; Riley, M. J.; Hitchman, M. A. *Inorg. Chem.* **1988**, *27*, 894.
(24) Beattie, I. R.; Gilson, T. R.; Ozin, G. A. *J. Chem. Soc. A* **1969**, 534.
(25) Riley, M. J.; Hitchman, M. A. *Inorg. Chem.* **1987**, *26*, 3205.
(26) McGinnety, J. A. *J. Am. Chem. Soc.* **1972**, *94*, 8406.

associated with the planar chromophore are resolvable in the *b* and *c* polarized spectra but only one in POL 2.

The spectra for the (010) crystal face of Cs_2CuCl_4 (overgrown onto a crystal of Zn_2CuCl_4) has been measured[27] at 20 K for light polarized parallel to the *a* and *c* axes. Two bands are resolvable in each polarization.

Finally, spectra for NBZP have been recorded,[15,23] at 18 and 290 K, on an absolute scale for light incident on the (100) crystal face and polarized parallel to *b* and *c*. Three bands are resolvable in each polarization at each temperature.

Fitting to the Vibronic + Static Model. CLF intensity analyses for all six $[CuCl_4]^{2-}$ chromophores have been performed independently but in a closely similar manner. Both static and vibronic sources of intensity were included for the nonplanar systems; only vibronic for the planar species. Static contributions in centrosymmetric systems do indeed yield vanishing intensity, as required and as checked explicitly.

All vibronic contributions relate to the three *ungerade* bends of the planar species, a_{2u}, b_{2u}, e_u; or to the four bends of the nonplanar complexes—ν_2, ν_3, ν_4, ν_7 (b_2, b_1, a_1, e) of Table 5. Restricting attention just to bends in this way means that all vibronic ${}^{L}t_{\lambda}^{\alpha}(Q)$ parameters are proportional to "underlying" static ${}^{L}t_{\lambda}$ parameters. Inclusion of stretching modes would require additional variables. The restriction is justified (a) by the bends invariably occurring with lower frequencies and hence higher amplitudes than the stretches, (b) by the ultimate success of this modeling for the present complexes as well as for others already published, and (c) by the good reproduction of the temperature dependences of those systems for which data is available.

Altogether therefore, the CLF intensity parametrization comprises ${}^{P}t_{\sigma}$, ${}^{F}t_{\sigma}$, ${}^{P}t_{\pi}$, and ${}^{F}t_{\pi}$, of which only three are freely variable when fitting intensity *distributions*. This three-parameter model was applied to the lowest temperature spectra of each chromophore and, for the planar species, for the two or three sets of ligand displacements described by the NCAs above. For each chromophore and for each NCA set, excellent reproduction of all intensity distributions were obtained. Intensity *t* parameters associated with the different NCA ligand displacements in the planar systems differed only slightly. All the fits were achieved easily with few computational iterations. In this respect, the contrast with the analyses using the earlier scheme—model IIA—was remarkable.

These successes were followed by an investigation of the temperature dependence of those spectra for which such data is available; namely, METH, CREAT, and NMPH. Analyses proceeded on the basis of the optimal *t* parameters determined for the lowest temperature spectra multiplied by appropriate factors expressing the variation of ligand displacements as functions of temperature and determined from the NCAs. No subsequent optimization of fits by variation of *t* parameters was made. In short, we sought to reproduce the temperature dependences of the various spectra by reference to the ligand dynamics alone. Reproduction of the experimental temperature dependences varies in quality with respect to the choice of NCA ligand displacement set (for the planar species). It is not good

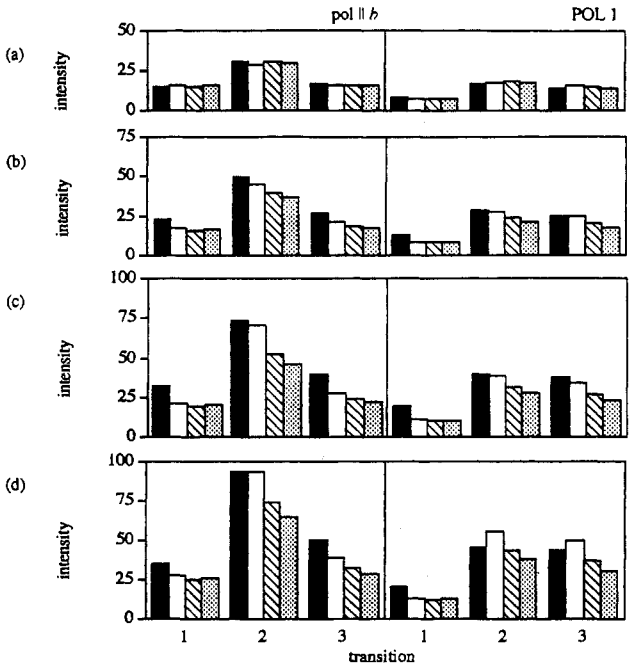

Figure 1. Comparison of observed (solid box) and calculated intensity distributions for NMPH using the three choices for the frequency of the inactive vibrational mode ν_4 shown in Table 3, (open box for choice i, hatched box for choice ii, and shaded box for choice iii) at (a) 10, (b) 77, (c) 120, and (d) 185 K.

Table 6. CLF Intensity Parameters Reproducing the Intensity Distribution in the Low Temperature Polarized Crystal Spectra of the $[CuCl_4]^{2-}$ Ions, Where Parameter Sets Correspond to the Calculations Using the b_{2u} Frequencies Labeled (i) in Table 3 and Estimated Errors Are Shown in Parentheses

system	${}^{P}t_{\sigma}$	${}^{F}t_{\sigma}$	${}^{P}t_{\pi}$	${}^{F}t_{\pi}$
METH[a]	10(±5)	64	14(±5)	56(±9)
CREAT[a]	19(±6)	69	21(±5)	62(±9)
NMPH	5(±5)	70	8(±5	65(±12)
NAEM	3(±5)	62	0(±5)	56(±9)
NBZP[a]	246	73(±15)	176(±20)	115(±15)
Cs_2CuCl_4	452	70(±20)	374(±44)	70(±20)

[a] Parameters in units of D × 10^{-2}. The parameters for the other systems are in arbitrary units of dipole moment, but scaled, as in the text.

at all for the choice (iii) corresponding to the value 105 cm^{-1} for the frequency of the b_{2u} bend in NMPH. Also, quite generally throughout the planar group of chromophores, reproduction of the temperature dependence of the intensity distributions *and* of these distributions at base temperature is significantly better for the choice ν_4 = 64 cm^{-1} rather than ν_4 = 88 cm^{-1}. Our analyses thus indicate that coupling between "orthogonal" Cl−Cu−Cl bends is significant and, except for the case of NMPH, favor the b_{2u} frequencies as determined directly *via* the coth rule over those calculated from NCA under the assumption $F_{22} = F_{44}$. Figure 1 compares the calculated temperature dependence of intensity with experiment for the three choices of the ν_4 frequency for NMPH.

Having favored choices i in this way, we therefore list optimal *t* parameters sets in detail for (i) only in Table 6 and display comparison of observed and calculated intensities in Table 7.

Comparisons with Earlier Analyses. Once the straightforward studies of vibrational frequencies by NCA were complete, the CLF analyses of "d−d" intensities were all simple, computationally brisk and essentially unique. These observations apply equally to the planar and non-planar chromophores; that is, to pure vibronic or to mixed vibronic/static sources of

(27) Ferguson, J. *J. Chem. Phys.* **1964**, *40*, 3406.
(28) Deeth, R. J.; Gerloch, M. *J. Chem. Soc., Dalton Trans.* **1986**, 1531.
(29) Nelson, H. C.; Simonsen, S. H.; Watt, G. W. *J. Chem. Soc., Chem. Commun.* **1979**, 632.
(30) Udupa, M. R.; Krebs, B. *Inorg. Chim. Acta* **1966**, *4*, 1.
(31) Harlow, R. L.; Wells, W. J., III; Watt, G. W.; Simonsen, S. H. *Inorg. Chem.* **1974**, *13*, 2106.
(32) Battaglia, L. P.; Bonamartini Corradi, A.; Marcotrigiano, G.; Menabue, L.; Pellacini, G. C. *Inorg. Chem.* **1982**, *21*, 3919.
(33) Antolini, L.; Menabue, L.; Pellacini, G. C.; Saladini, M. *Inorg. Chim. Acta* **1982**, *58*, 193.

Table 7. Observed Intensity Distributions in $[CuCl_4]^{2-}$ Ligand-Field Spectra Compared with Those Calculated Using the Parameter Sets of Table 6, Where Intensities are Quoted in D^2 cm^{-1} for METH, CREAT, NAEM, and NBZP but in Arbitrary Units Otherwise

	pol ∥ *b*		pol. ∥ *c*	
METH transition	obsd[a]	calcd	obsd[a]	calcd
ν_1	86	90	17	14
ν_2	221	228	80	59
ν_3	66	78	116	120
	pol. ∥ *b*		pol. ∥ *c*	
CREAT transition	obsd[a]	calcd	obsd[a]	calcd
ν_1	127	128	0	5
ν_2	284	284	35	44
ν_3	66	59	117	110
	pol. ∥ *b*		POL 1	
NMPH transition	obsd[a]	calcd	obsd[a]	calcd
ν_1	15	15	8	8
ν_2	30	29	16	18
ν_3	16	15	14	15

	pol. ∥ *b*		POL 2		pol. ∥ *c*	
NAEM transition	obsd[a]	calcd	obsd[a]	calcd	obsd[a]	calcd
ν_1		6		52		49
ν_2	46	70	270	250		260
ν_3	55	63	130	94	130	110

	pol. ∥ *b*		pol. ∥ *c*	
NBZP transition	obsd[b]	calcd	obsd[b]	calcd
ν_1	122	179	97	78
ν_2	1020	968	490	550
ν_3	590	550	1400	1390
	pol. ∥ *b*		pol. ∥ *c*	
Cs_2CuCl_4 transition	obsd[c]	calcd	obsd[c]	calcd
ν_2	30	30	27	27
$\nu_1 + \nu_3$	34	34	9	9

[a] 10 K spectrum. [b] 18 K spectrum. [c] 20 K spectrum.

intensity. Model IIB clearly provides a much more desirable analytical tool than the earlier, more cautious model IIA.

Our first analysis[2,3] of the intensity distribution in Cs_2CuCl_4 considered just static sources through model I. Two rather different sets of intensity parameter values afforded essentially equally good reproduction of the experimental data. Arguments for preferring one parametrization over the other, based on comparisons with the analyses of other tetrahalides and upon separate theoretical work, have been presented.[3] The present analysis, using model IIB and including a vibronic contribution, singles out the optimal parameter set given in Table 6. The essential uniqueness of this fit appears to derive from the inclusion of a (small) vibronic component as well as from the more mature facilities[34] currently offered by CAMMAG4 for the searching of polyparameter space. We note that the present fit corresponds closely with the preferred fit from the earlier analysis, obtained only after detailed correlation and outside reference.

In Figure 2, we present histograms illustrating the agreement between observed intensities in the lowest temperature spectrum for each system and those calculated with the optimal parameter values in Table 6, showing a breakdown into relative contributions enabled by the various bending modes and, where appropriate, the static field. These comparisons are made for individual spectral bands in different polarizations. Also

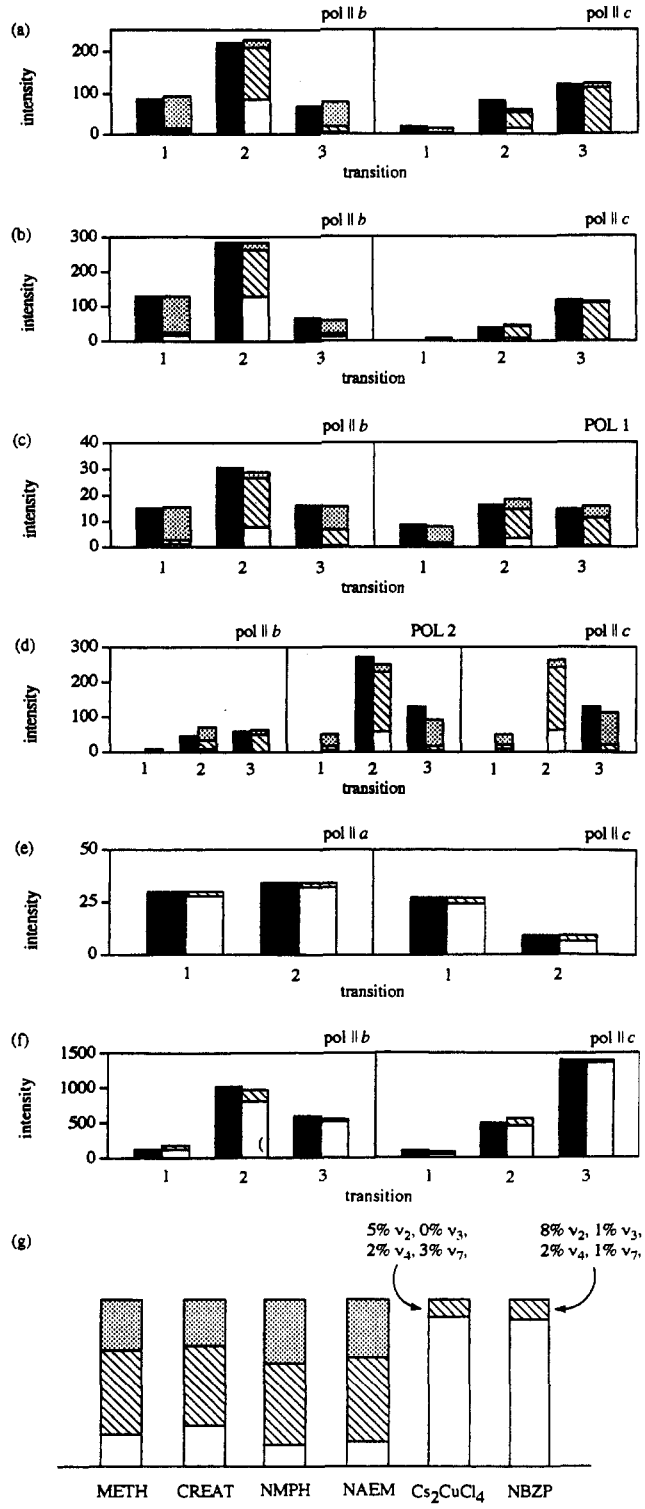

Figure 2. Comparison of the observed (solid box) intensity distributions in the lowest temperature spectrum with those calculated using the parameter sets of Table 6 for (a) METH, (b) CREAT, (c) NMPH, (d) NAEM, (e) Cs_2CuCl_4, and (f) NBZP. For the planar chromophores, the contributions of the three *ungerade* bending modes (open box for a_{2u}, hatched box for b_{2u}, and shaded box for e_u) to the intensity of each band are shown. The relative contributions to the total intensity from each mode are illustrated in part g. For the "tetrahedral" systems, the intensity generated through static mixing (open box) and by vibronic coupling (hatched box) is shown. Their relative contributions to the total intensity and an estimate of the importance of the various enabling vibrational modes is illustrated in part g.

(34) Dale, A. R.; Duer, M. J.; Fenton, N. D.; Gerloch, M.; McMeeking, R. F. CAMMAG4, a Fortran program suite. 1991.
(35) Deeth, R. J.; Gerloch, M. *Inorg. Chem.* **1985**, *24*, 1754.

Table 8. Comparison of the Average Energies (cm^{-1}) of the Vibrations Inducing Intensity in the Spectra of METH and CREAT from the Results of the Analyses Presented Here and from Those of Hitchman and McDonald[15,16] [HM], Where the Errors Estimated by Hitchman and McDonald Are Shown in Parentheses

	METH				CREAT			
	pol. ∥ *b*		pol. ∥ *c*		pol. ∥ *b*		pol. ∥ *c*	
transition	here	HM	here	HM	here	HM	here	HM
ν_1	172	200(25)			178	205(20)		
ν_2	108	100(10)	90	110(20)	112	110(20)	82	90(20)
ν_3	153	165(25)	70	62(6)	166	155(10)	65	64(4)

included is an equivalent breakdown of the total intensity for a given chromophore, corresponding to the sum of all observed bands in all polarizations. Our earlier analyses[11] for the planar $[CuCl_4]^{2-}$ chromophores suggested that reasonable reproduction of intensity distributions could be constructed with recognition of the b_{2u} bend alone. Reasons of physicality, to do with vibrational amplitudes, led us to prefer an alternative parametrization in terms of b_{2u} and e_u together. We were unable to assess any contribution from the a_{2u} bend. The intensity breakdowns in Figure 2 make clear that the completed vibronic model (IIB) recognizes significant contributions from all three bending modes. Those from b_{2u} are the largest, but not by a large factor. Those from a_{2u} are the smallest, though by no means insignificant.

McDonald and Hitchman[16] have calculated the average energies of the inducing modes for each band in the spectra of METH and CREAT from the temperature dependence of intensity. It is interesting to compare their results with the average energies of the inducing modes found using the present analyses. Each mode makes at least a small contribution to each band so that an average is found by weighting the frequencies of each mode by its relative contribution to the intensity of the band. The results, corresponding to the optimal parametrizations (i) for METH and CREAT are presented in Table 8. These values are based on the low temperature analyses where the resolution of the bands is likely to be the most accurate. McDonald and Hitchman's average energies were derived by application of the coth rule. Table 8 evidences generally excellent agreement between the two sets of mean energies except for those of ν_1. The results of McDonald and Hitchman rely on resolving the bands in the high temperature spectra. That band is poorly resolved in the ∥ *b* polarization for both chromophores. At the higher temperatures, it is little more than a shoulder on the side of the ν_2 band. McDonald[15] has commented that this may result in the band area of the ν_1 band being underestimated. The reported inducing mode mean energies are thus probably upper limits, so that the difference between McDonald and Hitchman's[16] results and our own are unlikely to be significant.

The ν_3 transition is only allowed in the *x,y* polarization (corresponding approximately to the ∥ *b* polarization in both METH and CREAT) by an inducing mode of e_u symmetry according to the vibronic selection rules for D_{4h} symmetry. McDonald and Hitchman calculate average frequencies for this transition of *ca.* 165 cm^{-1} and 155 cm^{-1} for METH and CREAT respectively. These are lower values than the frequencies of the observed e_u bending vibrations (ν_7) for these systems. They suggest that these differences arise by coupling to lattice modes of effective e_u symmetry. The values in Table 8, however, report McDonald and Hitchman's average frequencies without any such lattice contributions. That the average ν_3 frequencies calculated in the present work take values less than the observed e_u vibrational frequencies is owed to small, but significant, intensity contributions from the a_{2u} and b_{2u} modes to this transition that arise from the effects of spin-orbit coupling and, to a lesser extent, from the small geometrical departures of these chromophores from exact D_{4h} symmetry.

We suggest that considerable weight is to be attached to the present analyses particularly because of their straightforward and reasonably quantitative reproduction of the *temperature variations* of the spectral intensities. Within the earlier study, reproductions of these temperature dependences were achieved only by free variation of all ${}^{L}t_{\lambda}^{\alpha}(Q)$ parameters. Here, a much less free parametrization is employed such that electronic features (the ${}^{L}t_{\lambda}$ variables) are held in common for each temperature analysis; in short, the temperature dependences of the ligand-field intensities are ascribed totally to the temperature dependences of the vibrations as computed by NCA. Again, this self-consistency has been achieved by reference to bond bending alone. Our neglect of bond stretches appears, therefore, to be justified.

Analyses of Planar Platinum(II) and Palladium(II) Chromophores

Here we are concerned with the "d−d" spectra of $[PtCl_4]^{2-}$, $[PtBr_4]^{2-}$, and $[PdCl_4]^{2-}$ within the K_2PtCl_4 lattices. Much work has been done on these systems already, and our own study[12] of the intensity distributions in the platinum species summarizes the current position.

Analyses of the transition *energies* in these species, and of some substituted analogues,[36] reproduce experimental band frequencies well but with non-unique values of the CLF e_{λ} and interelectron repulsion parameters. The correlations within these optimal parameter sets are an unfortunate consequence of the high molecular symmetry and of the necessity to parametrize the full d^8 basis in these diamagnetic complexes. They have been reported[12,36] in full and are not repeated here. The eigenvectors associated with different parameter combinations within these correlations vary little, however, so that we find the subsequent intensity analyses to be virtually independent of the particular, exemplary, optimal parameter set chosen for any chromophore.

Within the approach of model IIA, contributions to the dynamic parity mixing from different bending vibrational modes are freely parametrized. With some difficulty—in terms of searches and iterations within the polyparameter space—a good, and essentially unique, account of the intensity distribution within the $[PtCl_4]^{2-}$ chromophore was achieved. A rather less unique reproduction of intensities emerged from the bromo analogue, partly due to the lack of thick crystal data that, in the chloro complex, defined the relative intensities of several weaker bands. The spectrum of $[PdCl_4]^{2-}$ shows only two resolvable bands in each polarization rather than the five in the platinum chromophores. Model IIA is grossly overparametrized in this case, rendering an analysis of the intensity distribution impossible by this approach. We now describe the wholly successful application of the complete vibronic approach, model IIB, to all three d^8 species.

NCA of Vibrational Frequencies. Vibrational frequencies for the normal modes in the platinum(II) and palladium(II) complexes are listed in Table 9. Appropriate NCAs have been reported previously, the results of which are confirmed using our program in order to determine the tangential displacements

(36) Bridgeman, A. J.; Gerloch, M. *J. Chem. Soc., Dalton Trans.* **1995**, 197.
(37) Hendra, P. J. *Spectrochim. Acta* **1967**, *23A*, 2871.
(38) Ferraro, J. R. *J. Chem. Phys.* **1970**, *53*, 117.
(39) Hendra, P. J. *J. Chem. Soc. A* **1967**, 1298.
(40) Fertel, J. H.; Perry, C. *J. Phys. Chem. Solids* **1965**, *26*, 1773.
(41) Harrison, T. G.; Patterson, H. H.; Godfery, J. J. *Inorg. Chem.* **1976**, *15*, 1291.

Table 9. Vibrational Frequencies (cm^{-1}) of the $[PtCl_4]^{2-}$, $[PtBr_4]^{2-}$ and $[PdCl_4]^{2-}$ Ions

vibration	symmetry	activity (IR/ Raman)	$[PtCl_4]^{2-}$ [37,38]	$[PtBr_4]^{2-}$ [39,40]	$[PdCl_4]^{2-}$ [38,39]
ν_1	a_{1g}	R	329	205	205
ν_2	a_{2u}	IR	173	135	135
ν_3	b_{2g}	R	194	125	125
ν_4	b_{2u}		{174}[a]	{83}[b]	{157}[a]
ν_5	b_{1g}	R	302	190	190
ν_6	e_u(stretch)	IR	325	232	232
ν_7	e_u(bend)	IR	195	135	135

[a] Inactive mode calculated by normal coordinate analysis by Harrison et al.[41] [b] Inactive mode calculated by normal coordinate analysis by Tranquille et al.[42]

Table 10. Symmetry Coordinate Force Constants (mdyn $Å^{-1}$) for $[PtCl_4]^{2-}$, $[PtBr_4]^{2-}$, and $[PdCl_4]^{2-}$

force constant	$[PtCl_4]^{2-}$	$[PtBr_4]^{2-}$	$[PdCl_4]^{2-}$
F_{11}	2.261	1.980	2.007
F_{22}	0.181	0.179	0.129
F_{33}	0.197	0.203	0.205
F_{44}	0.316	0.179	0.257
F_{55}	1.900	1.701	1.580
F_{66}	1.642	1.514	1.439
F_{67}	0.092	0.084	0.093
F_{77}	0.314	0.325	0.275

suffered by the ligands during bending vibrations. Alternative schemes for the unobservable ν_4 (b_{2u}) bend have been considered, depending on the neglect or otherwise of the interaction constant $f_{\theta\theta}$ (see Appendix). In contrast to the situation for the copper complexes, the lack of detailed measures of the temperature dependence of the ligand-field spectra precludes our forming any clear preferences for any one vibrational parametrization scheme; we have followed those of Harrison et al.[41] and of Tranquille and Forel.[42] Our subsequent vibronic analyses are reasonably insensitive to the choice. Table 10 lists force constants derived from these NCAs.

Intensity Analyses for the d^8 Species

K_2MX_4 (M = Pt(II), Pd(II); X = Cl, Br) are isomorphous,[43-47] crystallizing in the tetragonal space group *P4/mmm*. The MX_4^{2-} chromophores have exact D_{4h} symmetry. Single crystal "d–d" spectra have been recorded for light-polarized || *a* and || *c* crystal axes, corresponding to molecular in-plane (*xy*) and out-of-plane (*z*) polarizations, respectively. Five resolvable bands are available for each polarization for the platinum complexes[48,49] but only two for each polarization[50] for $[PdCl_4]^{2-}$.

As for the planar d^9 species above, the full vibronic approach of model IIB is parametrized by just the "underlying" static parameters ${}^Pt_\sigma$, ${}^Ft_\sigma$, ${}^Pt_\pi$, ${}^Ft_\pi$ of which only three are to be varied in fitting *relative* intensities. The contributions of all bending modes have been taken into account through the mean tangential displacements derived from the appropriate NCAs. Further, as for the d^9 chromophores, the analyses proceeded briskly, yielding good agreement with observed intensity distributions for essentially unique *t* parameter sets. These optimal parameter values are given in Table 11 and the quality of agreement between observed and calculated intensities is shown in Table 12. The relative contributions to the total intensities (i.e. summed over all bands in both polarizations) deriving from the three enabling *ungerade* bends are illustrated in Figure 3. As for the copper complexes, the contributions from the a_{2u} mode are the least; on the other hand, the e_u bend appears to be somewhat more effective than the b_{2u} in the d^8 systems.

Table 11. CLF Intensity Parameters (D × 10^{-2}) Reproducing the Intensity Distribution in the 15 K Polarized Crystal Spectra of the $[PtCl_4]^{2-}$, $[PtBr_4]^{2-}$, and $[PdCl_4]^{2-}$ Ions

param	$[PtCl_4]^{2-}$	$[PtBr_4]^{2-}$	$[PdCl_4]^{2-}$
${}^Pt_\sigma$	225	249	229
${}^Ft_\sigma$	142(±50)	281(±60)	46(±30)
${}^Pt_\pi$	0(±15)	0(±15)	0(±15)
${}^Ft_\pi$	247(±50)	411(±80)	286(±50)

Table 12. Observed and Calculated Intensity Distributions (in units of D^2 cm^{-1} × 10) in the 15 K Polarized Crystal Spectra of $[PtCl_4]^{2-}$, $[PtBr_4]^{2-}$ and $[PdCl_4]^{2-}$

		polarization *a* (*x*,*y*)		polarization *c* (*z*)	
band no.	range	obsd	calcd[a]	obsd	calcd[a]
		$[PtCl_4]^{2-}$			
1	16 000–19 000	4	9	4[d]	1
2	19 000–23 000	22	33	21	13
3	23 000–25 000	21	24	11[e]	25
4	25 000–28 000	41	24	0	0
5	28 000–31 000	115	99	129	140
		$[PtBr_4]^{2-}$			
1	15 000–17 500	9	11	0.1[d]	0.1
2	17 500–21 000	30	20	35	10
3	21 000–23 500	22	43	32[e]	35
4	23 500–25 500	63	67	0	0
5	25 500–29 000	138	132	126	137
		$[PdCl_4]^{2-}$			
1	15 000–20 000	8	6	3	3
2	20 000–25 000	318	317	103	106

[a] Using the "midrange" CLF energy parameters of ref 12; e_σ(Cl) = 11 980 cm^{-1}, e_π(Cl) = 2272 cm^{-1}, $2e_\sigma$(void) = −13 470 cm^{-1}, F_2 = 885 cm^{-1}, F_4 = 80 cm^{-1}, and ζ = 2365 cm^{-1}. [b] Using the "midrange" CLF energy parameters of ref 12: e_σ(Br) = 10 000 cm^{-1}, e_π(Cl) = 939 cm^{-1}, $2e_\sigma$(void) = −13 269 cm^{-1}, F_2 = 587 cm^{-1}, F_4 = 87 cm^{-1}, and ζ = 1730 cm^{-1}. [c] Using the "midrange" CLF energy parameters of ref 12: e_σ(Cl) = 9200 cm^{-1}, e_π(Cl) = 1276 cm^{-1}, $2e_\sigma$(void) = −13 103 cm^{-1}, F_2 = 550 cm^{-1}, F_4 = 50 cm^{-1}, and ζ = 550 cm^{-1}. [d] Weak bands given low weighting in analysis. [e] Broad bands given low weighting in analysis.

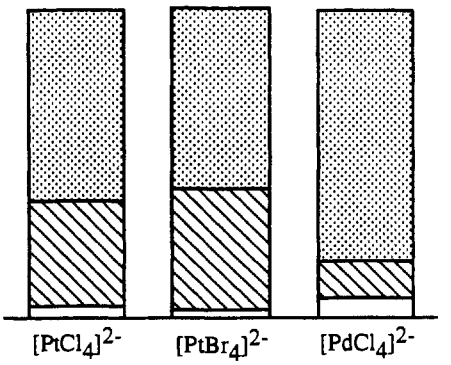

Figure 3. Relative contributions of the three *ungerade* bending modes (open box for a_{2u}, hatched box for b_{2u}, and shaded box for e_u) to the total intensity in the ligand-field spectra of $[PtCl_4]^{2-}$, $[PtBr_4]^{2-}$, and $[PdCl_4]^{2-}$.

(42) Tranquille, M.; Forel, M. H. *J. Chim. Phys. Physicochem. Biol.* **1971**, *68*, 471.
(43) Dickinson, R. G. *J. Am. Chem. Soc.* **1922**, *44*, 2404.
(44) Straritsky, E. *Anal. Chem.* **1956**, *28*, 915.
(45) Mais, R. H.; Owston, P. G.; Wood, A. M. *Acta Crystallogr.* **1972**, *28B*, 393.
(46) Kroening, R. F.; Rush, R. M.; Martin, D. S., Jr.; Clardy, J. C. *Inorg. Chem.* **1974**, *13*, 1366.
(47) Martin, D. S., Jr.; Bonte, J. L.; Rush, R. M.; Jacobsen, R. A. *Acta Crystallogr.* **1975**, *31B*, 2538.
(48) Martin, D. S., Jr.; Tucker, M. A.; Kassman, A. J. *Inorg. Chem.* **1965**, *4*, 1682. Amended: *Inorg. Chem.* **1966**, *5*, 1298.
(49) Martin, D. S., Jr. *Inorg. Chim. Acta Rev.* **1971**, *5*, 107.
(50) Rush, R. M.; Martin, D. S., Jr.; LeGrand, R. G. *Inorg. Chem.* **1975**, *14*, 2543.

Table 13. CLF "Static" Intensity Parameters (on Arbitrary Scale and Relative to $^{F}t_{\sigma} = 100$) for Tetrahedral $[MCl_4]^{2-}$ Species, after Reference 2

param	$^{P}t_{\sigma}$	$^{F}t_{\pi}$	$^{P}t_{\pi}$
$[CoCl_4]^{2-}$	54	65	110
$[NiCl_4]^{2-}$	155	120	125
$[CuCl_4]^{2-}$	300	40	400
	25	115	155

Conclusions

The new modeling of ligand-field intensity distributions incorporating static and vibronic sources of parity mixing, as appropriate, has provided excellent reproduction of all relevant experimental data available for nine $[MX_4]^{2-}$ species. In each case, straightforward searches of parameter space have yielded essentially unique values for the four intensity parameters, $^{P}t_{\sigma}$, $^{F}t_{\sigma}$, $^{P}t_{\pi}$, $^{F}t_{\pi}$, as given in Tables 6 and 11. We now consider these parameter values with respect to chromophore geometry and to the d^n configuration of the central metal.

First let us recall the t parameter values established by our earlier "static-only"—model I—approach[2] for the "tetrahedal" tetrachloro complexes of cobalt(II), nickel(II), and copper(II), as in Table 13. These values are given relative to $^{F}t_{\sigma} = 100$, as no absolute intensities had been recorded experimentally. As discussed in detail elsewhere,[2] P/F ratios—meaning $^{P}t_{\lambda}/^{F}t_{\lambda}$—are expected to reflect the relative polarizations of M−L bonds toward the metal such that the greater the ligand donation to the metal and/or the less the tangential compactness of the M−L bond, the greater the relative P-type contribution to intensity. In view of the increasing effective nuclear charge on the metal along the series Co(II), Ni(II), and Cu(II), the first of the two possible parameter sets for $[CuCl_4]^{2-}$ was strongly favored.[2] As noted before, the present analysis, incorporating vibronic as well as static parity mixing, has singled out that preferred fit. The relevant parameter values in Tables 13 and 6 differ a little, no doubt also as a result of our more mature parameter-space searching procedures,[34] but the expected trend is well confirmed.

Next consider the parameter sets in Table 6 for the planar copper(II) species discussed, METH, CREAT, NMPH, and NAEM. Those for METH, CREAT, and NAEM derive from measurements of crystal thickness and hence are given on an absolute scale. Those for NMPH are given relative to $^{F}t_{\sigma} = 70$ for the sake of comparison. Bearing in mind this freedom of scaling and the less good resolution of the NAEM spectra, we argue that the data in Table 6 present an essentially similar view of all four, planar, centric $[CuCl_4]^{2-}$ chromophores. The P/F ratio for the σ framework is on the order of 0.2.

The corresponding ratios, $^{P}t_{\sigma}/^{F}t_{\sigma}$, for the planar platinum species are 1.6 and 0.9 for $[PtCl_4]^{2-}$ and $[PtBr_4]^{2-}$ respectively. Furthermore, the values for $^{P}t_{\sigma}$ and (mostly) for $^{F}t_{\sigma}$ in Table 11 are absolutely larger than those for the d^9 planar species, by factors varying from 2 to 20. Both of these observations correlate well, we argue, with the magnitudes of nephelauxetic effects that have been observed in these, and related, species. Thus F_2/F_2(free ion) ratios for $[PtCl_4]^{2-}$ and $[PtBr_4]^{2-}$ chromophores have been estimated[12] to lie within the bounds 0.49−0.78 and 0.35−0.54, respectively. For the planar, low-spin d^7 complexes, Co(salen) and Co(clamben) (salen = *N,N'*-ethylenebis(salicylideneaminato) and clamben = *N,N'*-ethylenebis-(2-amino-5-chlorobenzylideneaminato)), F_2/F_2(free ion) values are 0.41 and 0.28 respectively.[51,52] In all these low-spin, d^7 and d^8 species, the $d_{x^2-y^2}$ orbital allows a closer approach[53] of the ligands along the local x and y axes. The consequently greater L→M electron donation results in larger ligand-field parameters (as compared, say, with analogous high-spin tetrahedral species) and greater nephelauxetic effects. In our present context, that unoccupied $d_{x^2-y^2}$ orbital is similarly reflected in the larger $^{P}t_{\sigma}/^{F}t_{\sigma}$ ratios. The smaller P/F ratios for $[PtBr_4]^{2-}$ with respect to $[PtCl_4]^{2-}$ does not conflict with the opposite trend for nephelauxetic effects as longer M−L bonds are otherwise associated with lower P/F ratios.

Similar reasoning applies when we compare $^{P}t_{\sigma}/^{F}t_{\sigma}$ ratios for the planar d^8 and d^9 species. The $d_{x^2-y^2}$ orbital houses no electrons in the d^8 species but one electron in the d^9. The steric activity of that nearly nonbonding electron tends to loosen the d^9 M−Cl bonds relative to those in the d^8 metals and this is reflected in the marked decrease in intensity P/F ratio from 1.6 for $[PtCl_4]^{2-}$ to 0.3 for $[CuCl_4]^{2-}$.

Having argued that trends in Z_{eff} account for the variation in P/F ratios for tetrahedral chloro Co(II), Ni(II), and Cu(II) complexes and that variations in the steric role of the open d shell rationalize those for the planar chloro Pt(II) and Cu(II) chromophores, we focus now on the marked differences between intensity parameters values for tetrahedral and planar chlorocuprates. Insofar that the Cu−Cl σ bonds are built from Cu 4s plus ligand σ functions, no first-order variation with Cl−Cu−Cl angle is to be expected. As the local $^{L}t_{\lambda}$ electric dipole transition moments are defined[1] so as to reflect the radial parts of d and bond orbitals, we similarly expect no first-order variation in either the magnitudes of the $^{L}t_{\lambda}$ parameters or in the $^{P}t_{\sigma}/^{F}t_{\sigma}$ ratio with respect to the Cl−Cu−Cl bond angle. On the other hand, however, contributions to the bond orbitals from Cu 4p functions are expected to vary with the geometry change from planar to tetrahedral $[CuCl_4]^{2-}$. No such contribution can occur at all in the centric planar environment. A $^{P}t_{\sigma}$ parameter relates[2] to the amount of p character in a ligand-field orbital, $(d + c\chi_{\text{lig}} + c'p)$. One contribution arises from the multipole expansion, say, of the ligand function χ_{lig}, onto the metal center. An f character contribution to $^{F}t_{\sigma}$ arises in a similar way. A second contribution arises from the admixture 4s−4p brokered by covalency with the ligands. Analogous 4s−4f mixing is expected to be trivial, of course. Altogether, therefore, we expect to see similar $^{F}t_{\sigma}$ parameter values in planar and tetrahedral $[CuCl_4]^{2-}$ species but larger $^{P}t_{\sigma}$ values in the noncentric tetrahedral environment than in the centrosymmetric planar one.

The values in Table 6 support this expectation. $^{F}t_{\sigma}$ values for those chromophores analyzed with respect to known absolute intensities—the planar METH, CREAT, and NAEM and the tetrahedrally distorted NBZP—take values close to 70 on the scale of the table. The value for $^{F}t_{\sigma}$ in NBZP, however, is ten or more times larger than in the planar species. Values for the even more nearly tetrahedral chromophore Cs_2CuCl_4 have not been established on an absolute scale (the spectra having been recorded[27] for the "overcoat" of Cs_2CuCl_4 on a crystal of Cs_2ZnCl_4) but are presented in Table 6, scaled such that $^{F}t_{\sigma} = 70$ by comparison with all other d^9 species here. The value of $^{P}t_{\sigma}$ appears then to reflect even greater participation of Cu 4p character in the bonding of this most tetrahedral complex.

Finally consider the intensity parameters relating to π bonding. Values of $^{F}t_{\pi}$ in Table 6 are essentially constant throughout the planar copper species. Those of $^{P}t_{\pi}$ vary between 0.14 and 0.33 times $^{F}t_{\pi}$, except for the NAEM complex. Given the estimated errors in the table and the less exacting nature of

(51) Duer, M. J. Ph.D. Thesis, University of Cambridge, U.K., 1988.
(52) Deeth, R. J.; Duer, M. J.; Gerloch, M. *Inorg. Chem.* **1987**, *26*, 2573.
(53) Gerloch, M.; Constable, E. C. C. *Transition Metal Chemistry*; VCH: Weinheim, Germany, 1994; Chapter 7.

the NAEM data, it seems fair to conclude that $^{P}t_{\pi}$ values vary only a little throughout the planar copper species and are, e.g., one-third of the magnitude of $^{F}t_{\pi}$. The $^{F}t_{\pi}$ value for the greatly flattened tetrahedral NBZP has roughly twice the magnitude of that for the planar species. Given the scaling that put $^{F}t_{\sigma} = 70$ for Cs_2CuCl_4, we find $^{F}t_{\pi}$ for this more nearly tetrahedral complex to be virtually the same as that for NBZP. At the same time, values of $^{P}t_{\pi}$ for the nonplanar chromophores are an order of magnitude greater than those for the planar molecules; and $^{P}t_{\pi}$ for the more tetrahedral Cs_2CuCl_4 is about twice that for NBZP. These trends in $^{P}t_{\pi}$ values, or indeed in the $^{P}t_{\pi}/^{F}t_{\pi}$ ratios, qualitatively mirror those for the analogous σ parameters. The reason is surely the same; namely, the increasing participation of the Cu 4p orbitals within the Cu–Cl bonds as planar geometry is progressively replaced by tetrahedral.

The greater magnitude of $^{F}t_{\pi}$ for the "tetrahedral" species relative to the planar appears to reflect differing σ and π bonding character in the Cu–Cl bonds as a function of geometry. Thus, in the planar species, the hole in the d shell is uniquely associated with the $d_{x^2-y^2}$ orbital and hence with Cu–Cl σ bonding. Good σ donation from the ligands is facilitated here. The same is not true for Cu–Cl π bonding which is sterically frustrated to a degree by the filled d_{xy}, d_{xz} and d_{yz} orbitals. In more tetrahedral geometry, the d shell hole is shared unequally between the various σ and π bonds. In short, we expect somewhat lesser σ donation and greater π donation from the chlorine ligands in the tetrahedral environment than in the planar. In some support of this idea are the greater $^{F}t_{\pi}$ values in the "tetrahedral" species.

It is obvious that the rationale proposed here for the observed trends in all intensity parameters will gain strength with the advent of more confirmatory data, and we shall bear this in mind. For the moment, however, it is worth observing that the values in Table 6, 11, and 13 form the largest body of intensity data on reasonably related chromophores available to date. The consistency of the values among closely similar chromophores and the chemical sense reflected in their variations with respect to geometry and d^n configuration surely lend confidence to the relevance and universality of our latest approach to the modeling of ligand-field spectra.

Appendix

The vibrations of a square-planar MX_4 species span the representations

$$\Gamma(D_{4h}) = a_{1g}\,(\text{stretch}) + b_{1g}\,(\text{stretch}) + b_{2g}\,(\text{in-plane bend}) + a_{2u}\,(\text{out-of-plane bend}) + b_{2u}\,(\text{out-of-plane bend}) + e_u\,(\text{stretch}) + e_u\,(\text{bend})$$

The internal coordinates required for a normal coordinate analysis of these chromophores are illustrated in Figure 4 for the case of $[PtCl_4]^{2-}$. The symmetry-adapted basis is then

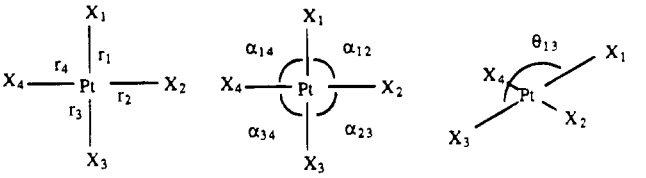

Figure 4. Internal coordinates used for normal coordinate analysis of MX_4 systems.

generated by a unitary transformation of these internal coordinates. Using the definitions in Figure 4, the symmetry coordinates are

$$S_1(a_{1g}) = (r_1 + r_2 + r_3 + r_4)/2,$$

$$S_2(a_{2u}) = R(\theta_{13} + \theta_{24})/\sqrt{2},$$

$$S_3(b_{2g}) = R(\alpha_{12} - \alpha_{23} + \alpha_{34} - \alpha_{41})/2,$$

$$S_4(b_{2u}) = R(\theta_{13} - \theta_{24})/\sqrt{2},$$

$$S_5(b_{1g}) = (r_1 - r_2 + r_3 - r_4)/2,$$

$$S_{6a}(e_u) = (r_1 - r_3)/\sqrt{2} \qquad S_{6b}(e_u) = (r_2 - r_4)/\sqrt{2},$$

$$S_{7a}(e_u) = R(\alpha_{12} - \alpha_{23} - \alpha_{34} + \alpha_{41})/2$$

$$S_{7b}(e_u) = R(\alpha_{12} + \alpha_{23} - \alpha_{34} - \alpha_{41})/2$$

where R is the equilibrium M–X bond length. The potential energy (or force constant) matrix in terms of these symmetry coordinates, $\boldsymbol{F}$, is similarly generated from the potential energy matrix in terms of the internal coordinates, $\boldsymbol{f}$. In the planar MX_4 systems for example, the force constants for the two out-of-plane modes, ν_2 and ν_4, are given by

$$F_{22} = f_\theta + f_{\theta\theta} \qquad F_{44} = f_\theta - f_{\theta\theta}$$

respectively. f_θ represents the force constant for the internal coordinates θ_{13} and θ_{24} and $f_{\theta\theta}$ represents the force constant for the interaction between the two motions. The tactic of setting $F_{22} = F_{44}$ is thus equivalent to the neglect of this interaction term. The matrix elements of $\boldsymbol{F}$ used in the text follow the enumeration of the modes given above. All calculations were performed using our extensively tested normal coordinate analysis program.[54]

IC950084Q

(54) Bridgeman, A. J.; Gerloch, M. VANAL, a Fortran computer program. 1993.